HEFAT2014
10th International Conference on Heat Transfer, Fluid Mechanics and Thermodynamics
14 - 16 July 2014
Orlando, Florida

CAN WE OBTAIN FIRST PRINCIPLE RESULTS FOR TURBULENCE STATISTICS?

Martin Oberlack[1,2,3], Andreas Rosteck[1] and Victor Avsarkisov[1]
[1]Chair of Fluid Dynamics, Department of Mechanical Engineering, TU Darmstadt, Germany
[2]Center of Smart Interfaces, TU Darmstadt, Germany
[3]GS Computational Engineering, TU Darmstadt, Germany
E-Mail: oberlack@fdy.tu-darmstadt.de

ABSTRACT

Text-book knowledge proclaims that Lie symmetries such as Galilean transformation lie at the heart of fluid dynamics. These important properties also carry over to the statistical description of turbulence, i.e. to the Reynolds stress transport equations and its generalisation, the multi-point correlation equations (MPCE). Interesting enough, the MPCE admit a much larger set of symmetries, in fact infinite dimensional, subsequently named statistical symmetries.

Most important, theses new symmetries have important consequences for our understanding of turbulent scaling laws. The symmetries form the essential foundation to construct exact solutions to the infinite set of MPCE, which in turn are identified as classical and new turbulent scaling laws. Examples on various classical and new shear flow scaling laws including higher order moments will be presented. Even new scaling have been forecasted from these symmetries and in turn validated by DNS.

Turbulence modellers have implicitly recognised at least one of the statistical symmetries as this is the basis for the usual log-law which has been employed for calibrating essentially all engineering turbulence models. An obvious conclusion is to generally make turbulence models consistent with the new statistical symmetries.

1 Introduction

The special importance of turbulence is determined by its ubiquity in innumerable natural and technical systems. Examples for natural turbulent flows are atmospheric flow and oceanic current which to calculate is a crucial point in climate research. Only with the advent of super computers it became apparent that the Navier-Stokes equations provide a very good continuum mechanical model for turbulent flows. Still, the exclusive and direct application of the Navier-Stokes equations to practical flow problems at high Reynolds numbers without invoking any additional assumptions is still several decades away.

However, in most applications it is not at all necessary to know all the detailed fluctuations of velocity and pressure present in turbulent flows but for the most part statistical measures are sufficient.

This was in fact the key idea of O. Reynolds who was the first to suggest a statistical description of turbulence. The Navier-Stokes equations, however, constitute a non-linear and, due to the pressure Poisson equation, a non-local set of equations. As an immediate consequence of this the equations for the mean or expectation values for velocity and pressure leads to an infinite set of statistical equations, or, if truncated at some level of statistics, an un-closed system is generated.

In order to obtain a much deeper insight into the statistical behavior of turbulence we presently apply Lie symmetry group theory to the full infinite set of statistical equations investigating various canonical turbulent flow situations.

This work is a continuation of that first reported in [1]. It extends the set of symmetries reported in [2] and [3] and is illustrated by application to various rotating channel flows and those with wall transpiration.

2 Equations of statistical turbulence theory

2.1 Navier-Stokes equations

The starting point of the analysis is the three dimensional Navier-Stokes equations for an incompressible fluid assuming

Newtonian fluid behaviour under constant density and viscosity conditions. In Cartesian tensor notation we have the continuity equation

$$\frac{\partial U_k}{\partial x_k} = 0 \tag{1}$$

and the momentum equation writes

$$\frac{\partial U_i}{\partial t} + U_k \frac{\partial U_i}{\partial x_k} = -\frac{1}{\rho}\frac{\partial P}{\partial x_i} + \nu \frac{\partial^2 U_i}{\partial x_k \partial x_k} \ , \ i = 1,2,3 . \tag{2}$$

where $t \in \mathbb{R}^+$, $\boldsymbol{x} \in \mathbb{R}^3$, $\boldsymbol{U} = \boldsymbol{U}(\boldsymbol{x},t)$ and $P = P(\boldsymbol{x},t)$ represent time, position vector, instantaneous velocity vector and pressure respectively. The density ρ and the kinematic viscosity ν are positive constants. Normalising pressure with constant density as $P^* = P/\rho$, and inserting it into (2), leads to a modified momentum equation and the asterisk is omitted from here on

$$\mathscr{M}_i(\boldsymbol{x}) = \frac{\partial U_i}{\partial t} + U_k \frac{\partial U_i}{\partial x_k} + \frac{\partial P}{\partial x_i} - \nu \frac{\partial^2 U_i}{\partial x_k \partial x_k} = 0 \ , \ \ i = 1,2,3 \tag{3}$$

where all terms have been collected on one side. Applying the divergence operator $\partial / \partial x_i$ to equation (3) and using the continuity equation (1) we obtain the Poisson equation for the pressure

$$\frac{\partial^2 P}{\partial x_k \partial x_k} = -\frac{\partial U_k}{\partial x_l}\frac{\partial U_l}{\partial x_k}. \tag{4}$$

2.2 Statistical averaging

In the following we define the classical Reynolds averaging. Though definitely mathematical more sound it is not intended to define the necessary multi-point probability density function to derive the multi-point equations in the subsequent section.

The quantity Z represents an arbitrary statistical variable, i.e. $\boldsymbol{U}$ and P, which in the following we also denote as *instantaneous value*. According to the classic definition by Reynolds all instantaneous quantities are decomposed into their mean and their fluctuation value

$$Z = \bar{Z} + z \ . \tag{5}$$

Here, the overbar denotes a statistically averaged quantity whereas the lower-case z denotes the fluctuation value of Z. The most general definition of statistically averaged quantity is given by an ensemble average operator $\mathscr{K}$

$$Z = \bar{Z}(\boldsymbol{x},t) = \mathscr{K}\left[Z(\boldsymbol{x},t)\right] = \lim_{N\to\infty}\left(\frac{1}{N}\sum_{n=1}^{N} Z_n(\boldsymbol{x},t)\right) \ . \tag{6}$$

In many cases a mean value in time is introduced for processes with a stationary mean:

$$\bar{Z}^{(T)}(\boldsymbol{x}) = \mathscr{L}^{(T)}\left[Z(\boldsymbol{x},t)\right] = \lim_{\tau\to\infty}\frac{1}{\tau}\int_{t-\frac{\tau}{2}}^{t+\frac{\tau}{2}} Z(\boldsymbol{x},t')\mathrm{d}t' \tag{7}$$

Its equivalence with the ensemble operator defined before is given by the Ergodic theorem. In problems with one or more homogeneous directions this property can be used to average in the particular direction. In turbulent flows through well-bounded chanals for example, averages are taken in layers parallel to the wall.

The definition of the mean value leads, according to the Reynolds decomposition, to the fluctuation value of Z

$$z = Z - \bar{Z} \ . \tag{8}$$

From the averaging operator above, several calculation rules may be derived e.g.

$$\begin{aligned}
\bar{z} &= 0 \ , \\
\overline{\overline{Z}} &= \overline{Z} \ , \\
\overline{Z_1 + Z_2} &= \overline{Z_1} + \overline{Z_2} \ , \\
\overline{\frac{\partial Z}{\partial s}} &= \frac{\partial \overline{Z}}{\partial s} \ , \\
\overline{\int Z \mathrm{d}s} &= \int \overline{Z} \mathrm{d}s \ , \\
\overline{\overline{Z}_{(1)}\overline{Z}_{(2)}\ldots\overline{Z}_{(m)} z_{(n)}} &= 0 \ , \\
\overline{z_{(1)} z_{(2)} \cdots z_{(k)}} &\neq 0 \ \text{ with } \ k > 1 \ ,
\end{aligned} \tag{9}$$

which in the following sub-sections will be employed to derive the multi-point equations.

2.3 Reynolds averaged transport equations

After $\boldsymbol{U}$ and P are decomposed according to the Reynolds decomposition, i.e. $\boldsymbol{U} = \bar{\boldsymbol{U}} + \boldsymbol{u}$ and $P = \bar{P} + p$, we gain an averaged versions of the continuity equation

$$\frac{\partial \bar{U}_k}{\partial x_k} = 0 \ , \tag{10}$$

the momentum equations

$$\frac{\partial \bar{U}_i}{\partial t} + \bar{U}_k \frac{\partial \bar{U}_i}{\partial x_k} = -\frac{\partial \bar{P}}{\partial x_i} + \nu \frac{\partial^2 \bar{U}_i}{\partial x_k \partial x_k} - \frac{\partial \overline{u_i u_k}}{\partial x_k} , \ i = 1,2,3 \tag{11}$$

and Poisson equation for the pressure

$$\frac{\partial^2 \bar{P}}{\partial x_k \partial x_k} = -\frac{\partial \bar{U}_k}{\partial x_l}\frac{\partial \bar{U}_l}{\partial x_k} - \frac{\partial \overline{u_k u_l}}{\partial x_l \partial x_k}. \tag{12}$$

At this point we observe the well-known closure problem of turbulence since, compared to the original set of equations, the unknown Reynolds stress tensor $\overline{u_i u_k}$ appeared. However, rather different from the classical approach we will not proceed with deriving the Reynolds stress tensor transport equation which contains additional four unclosed tensors. Instead the multi-point correlation approach is put forward the reason being twofold.

First, if the infinite set of correlation equations is considered the closure problem is somewhat bypassed. Second, the multi-point correlation delivers additional information on the turbulence statistics such as length scale information which may not be gained from the Reynolds stress tensor, which is a single-point approach.

For this we need the equations for the fluctuating quantities $\boldsymbol{u}$ and p which are derived by taking the differences between the averaged and the non-averaged equations, i.e. (1)/(10) and (3)/(11). The resulting fluctuation equations read

$$\frac{\partial u_k}{\partial x_k} = 0 \ , \tag{13}$$

and

$$\mathscr{N}_i(\boldsymbol{x}) = \frac{\bar{\mathrm{D}} u_i}{\bar{\mathrm{D}} t} + u_k \frac{\partial \bar{U}_i}{\partial x_k} - \frac{\partial \overline{u_i u_k}}{\partial x_k} + \frac{\partial u_i u_k}{\partial x_k} + \frac{\partial p}{\partial x_i} - \nu \frac{\partial^2 u_i}{\partial x_k \partial x_k} = 0, \ \ i = 1,2,3 \tag{14}$$

and extended by the corresponding Poisson equation for the pressure fluctuations

$$\frac{\partial^2 p}{\partial x_k \partial x_k} = -2 \frac{\partial \bar{U}_k}{\partial x_l}\frac{\partial u_l}{\partial x_k} + \frac{\partial^2 \overline{u_k u_l}}{\partial x_l \partial x_k} - \frac{\partial^2 u_k u_l}{\partial x_l \partial x_k}. \tag{15}$$

2.4 Multi-point correlation equations

It is considered that the idea of two- and multi-point equations in turbulence was first established in [4]. At the time it was assumed that all correlation equations of orders higher than two may be neglected. Theoretical considerations showed that all higher order correlations should be accounted for. Consequently, all multi-point correlation equations have been considered in the symmetry analysis that follows below.

Two different sets of multi-point correlation (MPC) equations will be derived below. The first is based on the instantaneous values of $\boldsymbol{U}$ and P while the second follows the classical notation based on the fluctuating quantities $\boldsymbol{u}$ and p.

2.4.1 MPC equations: instantaneous approach

In order to write the MPC equations in a very compact form, we introduce the following notation. The multi-point velocity correlation tensor of order $n+1$ is defined as follows:

$$H_{i_{\{n+1\}}} = H_{i_{(0)} i_{(1)} \dots i_{(n)}} = \overline{U_{i_{(0)}}(\boldsymbol{x}_{(0)}) \cdot \ldots \cdot U_{i_{(n)}}(\boldsymbol{x}_{(n)})} \ , \tag{16}$$

where the index i of the farthermost left quantity refers to its tensor character, while its superscript in curly brackets denotes the tensor order. The central term exemplifies this since a list of $n+1$ tensor indices is given where the index in parenthesis is a counter for the tensor order. It is important to mention that the index counter starts with 0 which is an advantage when introducing a new coordinate system based on the Euclidean distance of two or more space points. The mean velocity is given by the first order tensor as $H_{i_{\{1\}}} = H_{i_{(0)}} = \bar{U}_i$.

In some cases the list of indices is interrupted by one or more other indices which is pointed out by attaching the replaced value in square brackets to the index

$$H_{i_{\{n+1\}}[i_{(l)} \mapsto k_{(l)}]} = \overline{U_{i_{(0)}}(\boldsymbol{x}_{(0)}) \cdot \ldots \cdot U_{i_{(l-1)}}(\boldsymbol{x}_{(l-1)}) \cdot U_{k_{(l)}}(\boldsymbol{x}_{(l)}) U_{i_{(l+1)}}(\boldsymbol{x}_{(l+1)}) \cdot \ldots \cdot U_{i_{(n)}}(\boldsymbol{x}_{(n)})} \ . \tag{17}$$

This is further extended by

$$H_{i_{\{n+2\}}[i_{(n+1)} \mapsto k_{(l)}]}[\boldsymbol{x}_{(n+1)} \mapsto \boldsymbol{x}_{(l)}] = \overline{U_{i_{(0)}}(\boldsymbol{x}_{(0)}) \cdot \ldots \cdot U_{i_{(n)}}(\boldsymbol{x}_{(n)}) U_{k_{(l)}}(\boldsymbol{x}_{(l)})} \ , \tag{18}$$

where not only that index $i_{(n+1)}$ is replaced by $k_{(l)}$, but also that the independent variable $\boldsymbol{x}_{(n+1)}$ is replaced by $\boldsymbol{x}_{(l)}$. If indices are missing e.g. between $i_{(l-1)}$ and $i_{(l+1)}$ we define

$$H_{i_{\{n\}}[i_{(l)} \mapsto \emptyset]} = \overline{U_{i_{(0)}}(\boldsymbol{x}_{(0)}) \cdot \ldots \cdot U_{i_{(l-1)}}(\boldsymbol{x}_{(l-1)}) U_{i_{(l+1)}}(\boldsymbol{x}_{(l+1)}) \cdot \ldots \cdot U_{i_{(n)}}(\boldsymbol{x}_{(n)})} \ . \tag{19}$$

Finally, if pressure is involved we write

$$I_{i_{\{n\}}[l]} = \overline{U_{i_{(0)}}(\boldsymbol{x}_{(0)}) \cdot \ldots \cdot U_{i_{(l-1)}}(\boldsymbol{x}_{(l-1)}) P(\boldsymbol{x}_{(l)}) U_{i_{(l+1)}}(\boldsymbol{x}_{(l+1)}) \cdot \ldots \cdot U_{i_{(n)}}(\boldsymbol{x}_{(n)})} \ , \tag{20}$$

which is, considering all the above definitions, sufficient to derive the MPC equations from the equations of instantaneous velocity and pressure i.e. equation (1) and (3).

Applying the Reynolds averaging operator according to the sum below

$$\begin{aligned}
\mathscr{S}_{i_{\{n+1\}}}(\boldsymbol{x}_{(0)}, \ldots, \boldsymbol{x}_{(n)}) = & \\
& \overline{\mathscr{M}_{i_{(0)}}(\boldsymbol{x}_{(0)}) U_{i_{(1)}}(\boldsymbol{x}_{(1)}) \cdot \ldots \cdot U_{i_{(n)}}(\boldsymbol{x}_{(n)})} \\
& + \overline{U_{i_{(0)}}(\boldsymbol{x}_{(0)}) \mathscr{M}_{i_{(1)}}(\boldsymbol{x}_{(1)}) U_{i_{(2)}}(\boldsymbol{x}_{(2)}) \cdot \ldots \cdot U_{i_{(n)}}(\boldsymbol{x}_{(n)})} \\
& + \ldots \\
& + \overline{U_{i_{(0)}}(\boldsymbol{x}_{(0)}) \cdot \ldots \cdot U_{i_{(n-2)}}(\boldsymbol{x}_{(n-2)}) \mathscr{M}_{i_{(n-1)}}(\boldsymbol{x}_{(n-1)}) U_{i_{(n)}}(\boldsymbol{x}_{(n)})}
\end{aligned}$$

$$+\overline{U_{i_{(0)}}(\boldsymbol{x}_{(0)})\cdot\ldots\cdot U_{i_{(n-1)}}(\boldsymbol{x}_{(n-1)})\mathscr{M}_{i_{(n)}}(\boldsymbol{x}_{(n)})}\;, \tag{21}$$

we obtain the $\mathscr{S}$-equation which writes

$$\mathscr{S}_{i\{n+1\}}=\frac{\partial H_{i\{n+1\}}}{\partial t}+\sum_{l=0}^{n}\left[\frac{\partial H_{i\{n+2\}[i_{(n+1)}\mapsto k_{(l)}]}[\boldsymbol{x}_{(n+1)}\mapsto\boldsymbol{x}_{(l)}]}{\partial x_{k_{(l)}}}+\frac{\partial I_{i\{n\}[l]}}{\partial x_{i_{(l)}}}-\nu\frac{\partial^2 H_{i\{n+1\}}}{\partial x_{k_{(l)}}\partial x_{k_{(l)}}}\right]=0$$
$$\text{for}\quad n=1,\ldots,\infty\;. \tag{22}$$

In general equation (22) implies the full multi-point statistical information of the Navier-Stokes equations at the expense of dealing with an infinite dimensional chain of differential equations starting with order 2 i.e. $n=1$. The remarkable consequence of the derivation is that (22) is a linear equation which considerably simplifies the finding of Lie symmetries to be pointed out below.

From equation (1) a continuity equation for $H_{i\{n+1\}}$ and $I_{i\{n\}[l]}$ can be derived. This leads to

$$\frac{\partial H_{i\{n+1\}[i_{(l)}\mapsto k_{(l)}]}}{\partial x_{k_{(l)}}}=0\quad\text{for}\quad l=0,\ldots,n \tag{23}$$

and

$$\frac{\partial I_{i\{n\}[k][i_{(l)}\mapsto m_{(l)}]}}{\partial x_{m_{(l)}}}=0\quad\text{for}\quad k,l=0,\ldots,n\ \text{and}\ k\neq l\;. \tag{24}$$

At this point we adopt the classic notation of distance vectors. Accordingly the usual position vector $\boldsymbol{x}$ is employed and the remaining independent spatial variables are expressed as the difference of two position vectors $\boldsymbol{x}_{(l)}$ and $\boldsymbol{x}_{(0)}$. The coordinate transformation are

$$\boldsymbol{x}=\boldsymbol{x}_{(0)}\;,\qquad \boldsymbol{r}_{(l)}=\boldsymbol{x}_{(l)}-\boldsymbol{x}_{(0)}\quad\text{with}\quad l=1,\ldots,n. \tag{25}$$

and

$$\frac{\partial}{\partial x_{k_{(0)}}}=\frac{\partial}{\partial x_k}-\sum_{l=1}^{n}\frac{\partial}{\partial r_{k_{(l)}}}\,,\qquad \frac{\partial}{\partial x_{k_{(l)}}}=\frac{\partial}{\partial r_{k_{(l)}}}\quad\text{for}\quad l\geq 1\;. \tag{26}$$

For consistency the first index $i_{(0)}$ is replaced by i. Thus the indices of the tensor $\mathbf{H}_{\{n+1\}}$ are $H_{ii_{(1)}i_{(2)}\cdots i_{(n)}}$. Using the rules of transformation (25) and (26) the $\mathscr{S}$-equation leads to

$$\mathscr{S}_{i\{n+1\}}=\frac{\partial H_{i\{n+1\}}}{\partial t}+\frac{\partial H_{i\{n+2\}[i_{(n+1)}\mapsto k]}[\boldsymbol{x}_{(n+1)}\mapsto\boldsymbol{x}]}{\partial x_k}$$
$$-\sum_{l=1}^{n}\left[\frac{\partial H_{i\{n+2\}[i_{(n+1)}\mapsto k_{(l)}]}[\boldsymbol{x}_{(n+1)}\mapsto\boldsymbol{x}]}{\partial r_{k_{(l)}}}-\frac{\partial H_{i\{n+2\}[i_{(n+1)}\mapsto k_{(l)}]}[\boldsymbol{x}_{(n+1)}\mapsto\boldsymbol{r}_{(l)}]}{\partial r_{k_{(l)}}}\right]$$
$$+\frac{\partial I_{i\{n\}[0]}}{\partial x_i}+\sum_{l=1}^{n}\left(-\left.\frac{\partial I_{i\{n\}[0]}}{\partial r_{m_{(l)}}}\right|_{[m_{(l)}\mapsto i]}+\frac{\partial I_{i\{n\}[l]}}{\partial r_{i_{(l)}}}\right)$$
$$-\nu\left[\frac{\partial^2 H_{i\{n+1\}}}{\partial x_k\partial x_k}+\sum_{l=1}^{n}\left(-2\frac{\partial^2 H_{i\{n+1\}}}{\partial x_k\partial r_{k_{(l)}}}+\sum_{m=1}^{n}\frac{\partial^2 H_{i\{n+1\}}}{\partial r_{k_{(m)}}\partial r_{k_{(l)}}}+\frac{\partial^2 H_{i\{n+1\}}}{\partial r_{k_{(l)}}\partial r_{k_{(l)}}}\right)\right]=0$$
$$\text{for}\quad n=1,\ldots,\infty\;, \tag{27}$$

and the two continuity equations become

$$\frac{\partial H_{i\{n+1\}[i_{(0)}\mapsto k]}}{\partial x_k}-\sum_{j=1}^{n}\frac{\partial H_{i\{n+1\}[i_{(0)}\mapsto k_{(j)}]}}{\partial r_{k_{(j)}}}=0\;,$$
$$\frac{\partial H_{i\{n+1\}[i_{(l)}\mapsto k_{(l)}]}}{\partial r_{k_{(l)}}}=0\quad\text{for}\quad l=1,\ldots,n \tag{28}$$

and

$$\frac{\partial I_{i\{n\}[k][i\mapsto m]}}{\partial x_m}-\sum_{j=1}^{n}\frac{\partial I_{i\{n\}[k][i\mapsto m_{(j)}]}}{\partial r_{m_{(j)}}}=0 \tag{29}$$

for $k=1,\ldots,n$,

$$\frac{\partial I_{i\{n\}[k][i_{(l)}\mapsto m_{(l)}]}}{\partial r_{m_{(l)}}}=0 \tag{30}$$

for $k=0,\ldots,n$, $l=1,\ldots,n$, $k\neq l$.

2.4.2 MPC equations: fluctuation approach

In the present subsection we adopt the classical approach i.e. all correlation functions are based on the fluctuating quantities $\boldsymbol{u}$ and p as introduced by Reynolds and not on the full instantaneous quantities $\boldsymbol{U}$ and P as in the previous sub-section. Hence, similar to (16) we have the multi-point correlation for the fluctuation velocity

$$R_{i\{n+1\}}=R_{i_{(0)}i_{(1)}\cdots i_{(n)}}=\overline{u_{i_{(0)}}(\boldsymbol{x}_{(0)})\cdot\ldots\cdot u_{i_{(n)}}(\boldsymbol{x}_{(n)})}\;. \tag{31}$$

Further, all other correlations defined in sub-section 2.4.1 are defined accordingly i.e. equivalent to the definitions (17)-(20)

we respectively define $R_{i\{n+1\}[i_{(l)}\mapsto k_{(l)}]}$, $R_{i\{n+2\}[i_{(n+1)}\mapsto k_{(l)}]}[\boldsymbol{x}_{(n+1)}\mapsto \boldsymbol{x}_{(l)}]$, $R_{i\{n\}[i_{(l)}\mapsto\emptyset]}$ and $P_{i\{n\}[l]}$.

Finally, we define the correlation equation in analogy to (21) where $\mathscr{M}_i$ is replaced by the equation for the fluctuations (14) denoted by $\mathscr{N}_i$ and U_i and P are substituted by u_i and p. The resulting equation is denoted by $\mathscr{T}_{i\{n+1\}}$

$$\begin{aligned}\mathscr{T}_{i\{n+1\}} = \frac{\partial R_{i\{n+1\}}}{\partial t} + \sum_{l=0}^{n}\Bigg[&\bar{U}_{k_{(l)}}(\boldsymbol{x}_{(l)})\frac{\partial R_{i\{n+1\}}}{\partial x_{k_{(l)}}}\\ &+R_{i\{n+1\}[i_{(l)}\mapsto k_{(l)}]}\frac{\partial \bar{U}_{i_{(l)}}(\boldsymbol{x}_{(l)})}{\partial x_{k_{(l)}}}+\frac{\partial P_{i\{n\}[l]}}{\partial x_{i_{(l)}}}\\ &-\nu\frac{\partial^2 R_{i\{n+1\}}}{\partial x_{k_{(l)}}\partial x_{k_{(l)}}}-R_{i\{n\}[i_{(l)}\mapsto\emptyset]}\frac{\partial\overline{u_{i_{(l)}}u_{k_{(l)}}}(\boldsymbol{x}_{(l)})}{\partial x_{k_{(l)}}}\\ &+\frac{\partial R_{i\{n+2\}[i_{(n+1)}\mapsto k_{(l)}]}[\boldsymbol{x}_{(n+1)}\mapsto\boldsymbol{x}_{(l)}]}{\partial x_{k_{(l)}}}\Bigg]=0\\ &\text{for}\quad n=1,\ldots,\infty\ .\end{aligned} \tag{32}$$

The first tensor equation of this infinite chain propagates $R_{i\{2\}}$ which has a close link to the Reynolds stress tensor, i.e.

$$\lim_{x_{(k)}\to x_{(l)}} R_{i\{2\}} = \lim_{x_{(k)}\to x_{(l)}} R_{i_{(0)}i_{(1)}} = \overline{u_{i_{(0)}}u_{i_{(1)}}}(\boldsymbol{x}_{(l)})\quad \text{mit}\quad k\neq l\ , \tag{33}$$

which is the key unclosed quantity in the Reynolds stress transport equation (11). Here $x_{(k)}$ and $x_{(l)}$ can be arbitrary vectors out of $x_{(0)},\ldots,x_{(n)}$.

Also equation (32) implies all statistical information of the Navier-Stokes equations. However, apart from the latter simple relation to the Reynolds stress tensor it possesses the key disadvantage of being a *non-linear* infinite dimensional system of differential equations which make the extraction of Lie symmetries from this equation rather cumbersome. There are two essential sources of non-linearity in these equations. One is the known convection non-linearity which links the mean velocity to all correlation equations. The second source of non-linearity originates from the second row of equation (32). It is based on the fact that the gradient of the Reynolds stress tensor is contained in the equations of fluctuation. Hence, considering the following identity, this term is not equal to zero for turbulent flows and for multi-point correlation tensors of order higher than two

$$R_{i\{1\}[i_{(l)}\mapsto\emptyset]}=0\ . \tag{34}$$

As a direct consequence all multi-point correlation equations of order $n>1$ are coupled to the two-point correlation equation.

From equation (13) a continuity equation for $R_{i\{n+1\}}$ and $P_{i\{n\}[l]}$ can be derived. They have identical form to (23) and (24) for $H_{i\{n+1\}}$ and $I_{i\{n\}}$

$$\frac{\partial R_{i\{n+1\}[i_{(l)}\mapsto k_{(l)}]}}{\partial x_{k_{(l)}}}=0\quad\text{for}\quad l=0,\ldots,n \tag{35}$$

and

$$\frac{\partial P_{i\{n\}[k][i_{(l)}\mapsto m_{(l)}]}}{\partial x_{m_{(l)}}}=0\quad\text{for}\quad k,l=0,\ldots,n\quad\text{and}\quad k\neq l\ . \tag{36}$$

As above in 2.4.1 the classical difference vector notation (25) is adopted which leads to

$$\begin{aligned}\mathscr{T}_{i\{n+1\}}=&\frac{\bar{\mathrm{D}}R_{i\{n+1\}}}{\bar{\mathrm{D}}t}+\sum_{l=1}^{n}R_{i\{n+1\}[i_{(l)}\mapsto k_{(l)}]}\frac{\partial\bar{U}_{i_{(l)}}(\boldsymbol{x}_{(l)})}{\partial x_{k_{(l)}}}\\ &+\sum_{l=1}^{n}\left[\bar{U}_{k_{(l)}}(\boldsymbol{x}+\boldsymbol{r}_{(l)})-\bar{U}_{k_{(l)}}(\boldsymbol{x})\right]\frac{\partial R_{i\{n+1\}}}{\partial r_{k_{(l)}}}\\ &+R_{i\{n+1\}[i\mapsto k]}\frac{\partial\bar{U}_i(\boldsymbol{x})}{\partial x_k}+\frac{\partial P_{i\{n\}[0]}}{\partial x_i}\\ &+\sum_{l=1}^{n}\left(-\left.\frac{\partial P_{i\{n\}[0]}}{\partial r_{m_{(l)}}}\right|_{[m_{(l)}\mapsto i]}+\frac{\partial P_{i\{n\}[l]}}{\partial r_{i_{(l)}}}\right)-\nu\Bigg[\frac{\partial^2 R_{i\{n+1\}}}{\partial x_k\partial x_k}\\ &+\sum_{l=1}^{n}\left(-2\frac{\partial^2 R_{i\{n+1\}}}{\partial x_k\partial r_{k_{(l)}}}+\sum_{m=1}^{n}\frac{\partial^2 R_{i\{n+1\}}}{\partial r_{k_{(m)}}\partial r_{k_{(l)}}}+\frac{\partial^2 R_{i\{n+1\}}}{\partial r_{k_{(l)}}\partial r_{k_{(l)}}}\right)\Bigg]\\ &-R_{i\{n\}[i\mapsto\emptyset]}\frac{\partial\overline{u_iu_k}(\boldsymbol{x})}{\partial x_k}+\frac{\partial R_{i\{n+2\}[i_{(n+1)}\mapsto k]}[\boldsymbol{x}_{(n+1)}\mapsto\boldsymbol{x}]}{\partial x_k}\\ &-\sum_{l=1}^{n}\frac{\partial R_{i\{n+2\}[i_{(n+1)}\mapsto k_{(l)}]}[\boldsymbol{x}_{(n+1)}\mapsto\boldsymbol{x}]}{\partial r_{k_{(l)}}}\\ &-\sum_{l=1}^{n}R_{i\{n\}[i_{(l)}\mapsto\emptyset]}\frac{\partial\overline{u_{i_{(l)}}u_{k_{(l)}}}(\boldsymbol{x}_{(l)})}{\partial x_{k_{(l)}}}[\boldsymbol{x}_{(l)}\mapsto\boldsymbol{x}+\boldsymbol{r}_{(l)}]\\ &+\sum_{l=1}^{n}\frac{\partial R_{i\{n+2\}[i_{(n+1)}\mapsto k_{(l)}]}[\boldsymbol{x}_{(n+1)}\mapsto\boldsymbol{r}_{(l)}]}{\partial r_{k_{(l)}}}=0,\end{aligned} \tag{37}$$

for $n=1,\ldots,\infty$, and the two continuity equations transform alike.

$$\begin{aligned}&\frac{\partial R_{i\{n+1\}[i_{(0)}\mapsto k]}}{\partial x_k}-\sum_{j=1}^{n}\frac{\partial R_{i\{n+1\}[i_{(0)}\mapsto k_{(j)}]}}{\partial r_{k_{(j)}}}=0\ ,\\ &\frac{\partial R_{i\{n+1\}[i_{(l)}\mapsto k_{(l)}]}}{\partial r_{k_{(l)}}}=0\quad\text{for}\quad l=1,\ldots,n\end{aligned} \tag{38}$$

and

$$\frac{\partial P_{i\{n\}[k][i\mapsto m]}}{\partial x_m} - \sum_{j=1}^{n} \frac{\partial P_{i\{n\}[k][i\mapsto m_{(j)}]}}{\partial r_{m_{(j)}}} = 0 \quad \text{for} \quad k = 1, \ldots, n,$$
$$\frac{\partial P_{i\{n\}[k][i_{(l)}\mapsto m_{(l)}]}}{\partial r_{m_{(l)}}} = 0 \ \text{ for } \ k = 0, \ldots, n \ , \ \ l = 1, \ldots, n \ , \quad k \neq l \ . \tag{39}$$

From (5) - (9) it is apparent that there is a unique relation between the instantaneous (**H**, **I**) and the fluctuation approach (**R**, **P**) though the actual crossover is somewhat cumbersome in particular with increasing tensor order because they may only be given in recursive form. Since needed later we give the first relations

$$H_{i_{(0)}} = \bar{U}_{i_{(0)}} \tag{40}$$
$$H_{i_{(0)}i_{(1)}} = \bar{U}_{i_{(0)}}\bar{U}_{i_{(1)}} + R_{i_{(0)}i_{(1)}} \tag{41}$$
$$\begin{aligned} H_{i_{(0)}i_{(1)}i_{(2)}} &= \bar{U}_{i_{(0)}}\bar{U}_{i_{(1)}}\bar{U}_{i_{(2)}} + R_{i_{(0)}i_{(1)}}\bar{U}_{i_{(2)}} \\ &\quad + R_{i_{(0)}i_{(2)}}\bar{U}_{i_{(1)}} + R_{i_{(1)}i_{(2)}}\bar{U}_{i_{(0)}} + R_{i_{(0)}i_{(1)}i_{(2)}} \end{aligned} \tag{42}$$
$$\vdots \qquad \vdots$$

where the indices also refer to the spatial points as indicated.

With the identities (40)-(42) and alike equations it becomes apparent that, in contrast to the rather compact **H**-notation in equation (22), the MPC equation written in **R**-notation in equation (32) based on the mean and fluctuating quantities leads to a non-linear and non-local set of equations.

As a special case of the equations (32) we consider $n = 1$ including the $(\boldsymbol{x}, \boldsymbol{r})$-coordinate system (25) and we derive the equation for the two-point correlation tensor. To abbreviate the notation we introduce the following nomenclature:

$$R_{i\{2\}} = R_{ii_{(1)}} = R_{ij}(\boldsymbol{x}, \boldsymbol{r}, t) = \overline{u_i(\boldsymbol{x}, t)\, u_j(\boldsymbol{x} + \boldsymbol{r}, t)} \ . \tag{43}$$

In this case equation (32) reduces to

$$\begin{aligned} \mathscr{T}_{i\{2\}} &= \frac{\bar{\mathrm{D}} R_{ij}}{\bar{\mathrm{D}} t} + R_{kj}\, \frac{\partial \bar{U}_i(\boldsymbol{x}, t)}{\partial x_k} + R_{ik}\, \frac{\partial \bar{U}_j(\boldsymbol{x}, t)}{\partial x_k}\bigg|_{\boldsymbol{x}+\boldsymbol{r}} \\ &\quad + \left[\bar{U}_k(\boldsymbol{x} + \boldsymbol{r}, t) - \bar{U}_k(\boldsymbol{x}, t)\right] \frac{\partial R_{ij}}{\partial r_k} + \frac{\partial \overline{pu}_j}{\partial x_i} - \frac{\partial \overline{pu}_j}{\partial r_i} \\ &\quad + \frac{\partial \overline{u_i p}}{\partial r_j} - \nu \left[\frac{\partial^2 R_{ij}}{\partial x_k \partial x_k} - 2\, \frac{\partial^2 R_{ij}}{\partial x_k \partial r_k} + 2\, \frac{\partial^2 R_{ij}}{\partial r_k \partial r_k}\right] \\ &\quad + \frac{\partial R_{(ik)j}}{\partial x_k} - \frac{\partial}{\partial r_k}\left[R_{(ik)j} - R_{i(jk)}\right] = 0 \ . \end{aligned} \tag{44}$$

The quantities $\overline{pu}_j$, $\overline{u_i p}$ and $R_{(ik)j}$, $R_{i(jk)}$ are respectively special cases of $P_{i\{n\}[k]}$ and $R_{i\{n+2\}[i_{(n+1)}\mapsto k_{(l)}]}[\boldsymbol{x}_{(n+1)} \mapsto \boldsymbol{r}_{(l)}]$ and defined as

$$\begin{aligned} \overline{pu}_j(\boldsymbol{x}, \boldsymbol{r}, t) &= \overline{p(\boldsymbol{x}, t)\, u_j(\boldsymbol{x} + \boldsymbol{r}, t)} \\ \overline{u_i p}(\boldsymbol{x}, \boldsymbol{r}, t) &= \overline{u_i(\boldsymbol{x}, t)\, p(\boldsymbol{x} + \boldsymbol{r}, t)} \\ R_{(ik)j} &= \overline{u_i(\boldsymbol{x}, t)\, u_k(\boldsymbol{x}, t)\, u_j(\boldsymbol{x} + \boldsymbol{r}, t)} \\ R_{i(jk)} &= \overline{u_i(\boldsymbol{x}, t)\, u_j(\boldsymbol{x} + \boldsymbol{r}, t)\, u_k(\boldsymbol{x} + \boldsymbol{r}, t)} \ . \end{aligned} \tag{45}$$

For the two-point case the continuity equations take the form

$$\frac{\partial R_{ij}}{\partial x_i} - \frac{\partial R_{ij}}{\partial r_i} = 0 \ , \quad \frac{\partial R_{ij}}{\partial r_j} = 0 \ , \tag{46}$$

$$\frac{\partial R_{i(jk)}}{\partial x_i} - \frac{\partial R_{i(jk)}}{\partial r_i} = 0 \ , \quad \frac{\partial R_{(ik)j}}{\partial r_j} = 0 \ , \tag{47}$$

and

$$\frac{\partial \overline{pu}_i}{\partial r_i} = 0 \ , \quad \frac{\partial \overline{u_j p}}{\partial x_j} - \frac{\partial \overline{u_j p}}{\partial r_j} = 0. \tag{48}$$

The non-locality of the two- and multi-point correlation equations is most obvious when we use the commutation of the two-point correlation tensor. Given $\overline{u_i(\boldsymbol{x}_{(0)})u_j(\boldsymbol{x}_{(1)})} = \overline{u_j(\boldsymbol{x}_{(1)})u_i(\boldsymbol{x}_{(0)})}$ with equation (25) leads to the functional relations

$$R_{ij}(\boldsymbol{x}, \boldsymbol{r}; t) = R_{ji}(\boldsymbol{x} + \boldsymbol{r}, -\boldsymbol{r}; t) \tag{49}$$

and, similarly, to

$$R_{(ik)j}(\boldsymbol{x}, \boldsymbol{r}; t) = R_{j(ik)}(\boldsymbol{x} + \boldsymbol{r}, -\boldsymbol{r}; t) \ , \tag{50}$$

$$\overline{pu}_j(\boldsymbol{x}, \boldsymbol{r}; t) = \overline{u_j p}(\boldsymbol{x} + \boldsymbol{r}, -\boldsymbol{r}; t) \ . \tag{51}$$

Analogous identities can be derived for all other two- and multi-point correlation tensors.

3 Symmetries of statistical transport equations

In the present section we first revisit the Lie symmetries of the Euler and Navier-Stokes equations. In turn they will all be transferred to its corresponding ones for the MPC equations. In the second part we show that the MPC equations admit even more Lie symmetries which are not reflected in the original Euler and Navier-Stokes equations.

Both sets of symmetries will finally be employed in section 4 to show that classical and new scaling laws may not be determined from the classical symmetries alone but essentially rely on the new symmetries which we will call *statistical symmetries*.

In order to appreciate the analysis on Lie symmetries below we will define its basic concepts including that of *invariant solutions* which in the fluid mechanics community is usually referred to as self-similar solution though this in principle is limited to invariant solutions with certain scaling properties involved. In the turbulence community these types of solutions are usually denoted *turbulent scaling laws* though there they are in most cases not solutions of equations derived from first principles.

Suppose the system of partial differential equations under investigation is given by

$$\boldsymbol{F}(\boldsymbol{y},\boldsymbol{z},\boldsymbol{z}^{(1)},\boldsymbol{z}^{(2)},\dots)=0, \tag{52}$$

where $\boldsymbol{y}$ and $\boldsymbol{z}$ are the independent and the dependent variables respectively and $\boldsymbol{z}^{(n)}$ refers to all n^{th}-order derivatives of any component of $\boldsymbol{z}$ with respect to any component of $\boldsymbol{y}$. A transformation

$$\boldsymbol{y}=\phi(\boldsymbol{y}^*,\boldsymbol{z}^*) \quad \text{and} \quad \boldsymbol{z}=\psi(\boldsymbol{y}^*,\boldsymbol{z}^*) \tag{53}$$

is called a *symmetry* or *symmetry transformation* of the equation (52) if the following equivalence holds

$$\boldsymbol{F}(\boldsymbol{y},\boldsymbol{z},\boldsymbol{z}^{(1)},\dots)=0 \quad \Leftrightarrow \quad \boldsymbol{F}(\boldsymbol{y}^*,\boldsymbol{z}^*,\boldsymbol{z}^{*(1)},\dots)=0, \tag{54}$$

i.e. the transformation (53) substituted into (52) does not change the form of equation (52) if written in the new variables $\boldsymbol{y}^*$ and $\boldsymbol{z}^*$.

To illustrate this concept consider the 1D heat equation

$$\frac{\partial T}{\partial t}=\frac{\partial^2 T}{\partial x^2} \tag{55}$$

which, beside four other symmetries, admits the two scaling symmetries

$$t^*=\mathrm{e}^{2\alpha_1}t,\ \ x^*=\mathrm{e}^{\alpha_1}x,\ \ T^*=\mathrm{e}^{\alpha_2}T, \tag{56}$$

with the two independent group parameter $(\alpha_1,\alpha_2)\in\mathbb{R}$. For brevity the underlying two symmetries are presently combined into one transformation (56). It is evident that condition (54) is fulfilled since the implementation of (56) into (55) leaves the equation invariant if written in the new variables denoted by $*$.

A second concept which will be heavily relied on is that of an *invariant*. It refers to quantities that do not change structure under a given symmetry i. e.

$$I(\boldsymbol{y},\boldsymbol{z})=I(\phi(\boldsymbol{y}^*,\boldsymbol{z}^*),\psi(\boldsymbol{y}^*,\boldsymbol{z}^*))=I(\boldsymbol{y}^*,\boldsymbol{z}^*) \tag{57}$$

or in other words the form of I is invariant under the transformation. This may easily be clarified using the two-parameter symmetry (56). Beside others, in fact infinitely many, we may define and easily prove the existence of the two subsequent invariants

$$\delta=\frac{x}{\sqrt{t}}=\frac{x^*}{\sqrt{t^*}},\quad \Delta=\frac{T}{t^{\frac{\alpha_2}{2\alpha_1}}}=\frac{T^*}{t^{*\frac{\alpha_2}{2\alpha_1}}}. \tag{58}$$

as the insertion of (56) in δ and Δ in (58) shows the invariance of the latter quantities

The final concept in this context is that of an *invariant solution*. This concept implies that the invariants may be taken as new dependent and independent variables which in turn leads to a reduction of the number of the independent variables often referred to as symmetry reduction. It is this property of self-similar solutions which is profitable for some further analysis as fewer dimensions are involved.

For the example of the heat equation above we introduce δ and Δ as new independent and dependent variables respectively, i.e. we implement its definitions (58) into (55) and obtain the reduced differential equation

$$\frac{\mathrm{d}^2\Delta}{\mathrm{d}\delta^2}+\frac{1}{2}\delta\frac{\mathrm{d}\Delta}{\mathrm{d}\delta}-\frac{\alpha_2}{2\alpha_1}\Delta=0. \tag{59}$$

It should be noted that the actual computation of the symmetries such as (56), the invariants such as (58) and the invariant solutions is extremely simplified if the infinitesimal form of the symmetry is invoked [see 5]. This has been left out in the present contribution.

3.1 Symmetries of the Euler and Navier-Stokes equations

The Euler equations, i.e. equation (1) and (3) with $\nu=0$ admit a ten-parameter symmetry group,

$$\begin{aligned}
T_1:&\ t^*=t+k_1,\ \ \boldsymbol{x}^*=\boldsymbol{x},\ \ \boldsymbol{U}^*=\boldsymbol{U},\ \ P^*=P,\\
T_2:&\ t^*=t,\ \ \boldsymbol{x}^*=\mathrm{e}^{k_2}\boldsymbol{x},\ \ \boldsymbol{U}^*=\mathrm{e}^{k_2}\boldsymbol{U},\ \ P^*=\mathrm{e}^{2k_2}P,\\
T_3:&\ t^*=\mathrm{e}^{k_3}t,\ \ \boldsymbol{x}^*=\boldsymbol{x},\ \ \boldsymbol{U}^*=\mathrm{e}^{-k_3}\boldsymbol{U},\ \ P^*=\mathrm{e}^{-2k_3}P,\\
T_4-T_6:&\ t^*=t,\ \ \boldsymbol{x}^*=\mathbf{a}\cdot\boldsymbol{x},\ \ \boldsymbol{U}^*=\mathbf{a}\cdot\boldsymbol{U},\ \ P^*=P,\\
T_7-T_9:&\ t^*=t,\ \ \boldsymbol{x}^*=\boldsymbol{x}+\boldsymbol{f}(t),\ \ \boldsymbol{U}^*=\boldsymbol{U}+\frac{\mathrm{d}\boldsymbol{f}}{\mathrm{d}t},\\
&\quad P^*=P-\boldsymbol{x}\cdot\frac{\mathrm{d}^2\boldsymbol{f}}{\mathrm{d}t^2},\\
T_{10}:&\ t^*=t,\ \ \boldsymbol{x}^*=\boldsymbol{x},\ \ \boldsymbol{U}^*=\boldsymbol{U},\ \ P^*=P+f_4(t)\ ,
\end{aligned} \tag{60}$$

where k_1-k_3 are independent group-parameters, $\mathbf{a}$ denotes a constant rotation matrix with the properties $\mathbf{a}\cdot\mathbf{a}^\mathsf{T}=\mathbf{a}^\mathsf{T}\cdot\mathbf{a}=\mathbf{I}$ and

$|\mathbf{a}|=1$. Moreover $\boldsymbol{f}(t)=(f_1(t),f_2(t),f_3(t))^{\mathsf{T}}$ with twice differentiable functions f_1-f_3 and $f_4(t)$ may have arbitrary time dependence.

Each of the symmetries has a distinct physical meaning. T_1 means time translation i.e. any physical experiment is independent of the actual starting point. T_4-T_6 designate rotation invariance which refers to the possibility to let an experiment undergo a fixed rotation without changing physics. Note, that this does *not* mean moving into a rotating system since this does significantly change physics and hence is not a symmetry. The symmetries T_7-T_9 comprise translational invariance in space for constant f_1-f_3 as well as the classical Galilei group if f_1-f_3 are linear in time. These are key properties of classical mechanics referring to the fact that physics is independent of the location or if moved at a constant speed. In its rather general form T_7-T_9 and T_{10} are direct consequences of an incompressible flow and do not have a counterpart in the case of compressible flows. The complete record of all point-symmetries (60) was first published by Pukhnachev [6].

Invoking a formal transfer from Euler to the Navier-Stokes equations symmetry properties change and a recombination of the two scaling symmetries T_2 and T_3 is observed

$$T_{NaSt}:\quad t^*=\mathrm{e}^{2k_4}t,\ \ \boldsymbol{x}^*=\mathrm{e}^{k_4}\boldsymbol{x},\ \ \boldsymbol{U}^*=\mathrm{e}^{-k_4}\boldsymbol{U},\ \ P^*=\mathrm{e}^{-2k_4}P, \tag{61}$$

while the remaining groups stay unaltered.

It should be noted that additional symmetries exist for dimensional restricted cases such as plane or axisymmetric flows [see 7, 8].

3.2 Symmetries of the MPC implied by Euler and Navier-Stokes symmetries

Adopting the classical Reynolds notation first, where the instantaneous quantities are split into mean and fluctuating values, we may directly derive from (60)

$$\begin{aligned}
\bar{T}_1:\ & t^*=t+k_1,\ \ \boldsymbol{x}^*=\boldsymbol{x},\ \ \boldsymbol{r}^*_{(l)}=\boldsymbol{r}_{(l)},\ \ \bar{\boldsymbol{U}}^*=\bar{\boldsymbol{U}},\\
& \bar{P}^*=\bar{P},\ \ \mathbf{R}^*_{\{n\}}=\mathbf{R}_{\{n\}},\ \ \mathbf{P}^*_{\{n\}}=\mathbf{P}_{\{n\}},\\
\bar{T}_2:\ & t^*=t,\ \ \boldsymbol{x}^*=\mathrm{e}^{k_2}\boldsymbol{x},\ \ \boldsymbol{r}^*_{(l)}=\mathrm{e}^{k_2}\boldsymbol{r}_{(l)},\ \ \bar{\boldsymbol{U}}^*=\mathrm{e}^{k_2}\bar{\boldsymbol{U}},\\
& \bar{P}^*=\mathrm{e}^{2k_2}\bar{P},\ \ \mathbf{R}^*_{\{n\}}=\mathrm{e}^{nk_2}\mathbf{R}_{\{n\}},\mathbf{P}^*_{\{n\}}=\mathrm{e}^{(n+2)k_2}\mathbf{P}_{\{n\}},\\
\bar{T}_3:\ & t^*=\mathrm{e}^{k_3}t,\ \ \boldsymbol{x}^*=\boldsymbol{x},\ \ \boldsymbol{r}^*_{(l)}=\boldsymbol{r}_{(l)},\ \ \bar{\boldsymbol{U}}^*=\mathrm{e}^{-k_3}\bar{\boldsymbol{U}},\\
& \bar{P}^*=\mathrm{e}^{-2k_3}\bar{P},\ \ \mathbf{R}^*_{\{n\}}=\mathrm{e}^{-nk_3}\mathbf{R}_{\{n\}},\\
& \mathbf{P}^*_{\{n\}}=\mathrm{e}^{-(n+2)k_3}\mathbf{P}_{\{n\}},\\
\bar{T}_4\text{–}\bar{T}_6:\ & t^*=t,\ \ \boldsymbol{x}^*=\mathbf{a}\cdot\boldsymbol{x},\ \ \boldsymbol{r}^*_{(l)}=\boldsymbol{r}_{(l)},\ \ \bar{\boldsymbol{U}}^*=\mathbf{a}\cdot\bar{\boldsymbol{U}},\ \ \bar{P}^*=\bar{P},\\
& \mathbf{R}^*_{\{n\}}=\mathbf{A}_{\{n\}}\otimes\mathbf{R}_{\{n\}},\ \ \mathbf{P}^*_{\{n\}}=\mathbf{A}_{\{n\}}\otimes\mathbf{P}_{\{n\}},\\
\bar{T}_7\text{–}\bar{T}_9:\ & t^*=t,\ \ \boldsymbol{x}^*=\boldsymbol{x}+\boldsymbol{f}(t),\ \ \boldsymbol{r}^*_{(l)}=\boldsymbol{r}_{(l)},\ \ \bar{\boldsymbol{U}}^*=\bar{\boldsymbol{U}}+\frac{\mathrm{d}\boldsymbol{f}}{\mathrm{d}t},\\
& \bar{P}^*=\bar{P}-\boldsymbol{x}\cdot\frac{\mathrm{d}^2\boldsymbol{f}}{\mathrm{d}t^2},\ \ \mathbf{R}^*_{\{n\}}=\mathbf{R}_{\{n\}},\ \ \mathbf{P}^*_{\{n\}}=\mathbf{P}_{\{n\}},\\
\bar{T}_{10}:\ & t^*=t\ ,\ \ \boldsymbol{x}^*=\boldsymbol{x},\ \ \boldsymbol{r}^*_{(l)}=\boldsymbol{r}_{(l)},\ \ \bar{\boldsymbol{U}}^*=\bar{\boldsymbol{U}},\\
& \bar{P}^*=\bar{P}+f_4(t),\ \ \mathbf{R}^*_{\{n\}}=\mathbf{R}_{\{n\}},\ \ \mathbf{P}^*_{\{n\}}=\mathbf{P}_{\{n\}},
\end{aligned} \tag{62}$$

where all function and parameter definitions are adopted from 3.1 and $\mathbf{A}$ is a concatenation of rotation matrices as $A_{i_{(0)}j_{(0)}i_{(1)}j_{(1)}\dots i_{(n)}j_{(n)}}=a_{i_{(0)}j_{(0)}}a_{i_{(1)}j_{(1)}}\dots a_{i_{(n)}j_{(n)}}$.

The latter symmetries may also be transformed into the $\mathbf{H}$-notation. This will be omitted for briefness and also because the turbulent scaling laws to be derived and discussed below are rarely considered in this notation.

3.3 Statistical symmetries of the MPC equations

The concept of an extended set of symmetries for the MPC equation in the form (22) or (32) may e.g. be taken from [9] and [10]. Its importance was not observed therein - rather it was stated that they may be mathematical artifacts of the averaging process and probably physically irrelevant. The set of new symmetries was first presented and its key importance for turbulence recognised in [1] and later extended in [2].

The actual finding of symmetries of the non-rotating MPC is rather difficult since an infinite system of equations has to be analyzed. For this task, however, it is considerably easier to investigate the linear $\mathbf{H}$-$\mathbf{I}$-system (22)-(24) rather than the non-linear $\mathbf{R}$-$\mathbf{P}$-system (32)-(36). However, since the latter formulation is more common, the symmetries will finally be re-written in this notation.

This entire new set of symmetries for the $\mathbf{H}$-$\mathbf{I}$-system (22)-(24) can be separated in three distinct sets of symmetries

$$\begin{aligned}
\bar{T}'_1:\ & t^*=t,\ \ \boldsymbol{x}^*=\boldsymbol{x},\ \ \boldsymbol{r}^*_{(l)}=\boldsymbol{r}_{(l)}+\boldsymbol{k}_{(l)},\\
& \mathbf{H}^*_{\{n\}}=\mathbf{H}_{\{n\}},\ \ \mathbf{I}^*_{\{n\}}=\mathbf{I}_{\{n\}},
\end{aligned} \tag{63}$$

$$\begin{aligned}
\bar{T}'_{2_{\{n\}}}:\ & t^*=t,\ \ \boldsymbol{x}^*=\boldsymbol{x},\ \ \boldsymbol{r}^*_{(l)}=\boldsymbol{r}_{(l)},\\
& \mathbf{H}^*_{\{n\}}=\mathbf{H}_{\{n\}}+\mathbf{C}_{\{n\}},\ \ \mathbf{I}^*_{\{n\}}=\mathbf{I}_{\{n\}}+\mathbf{D}_{\{n\}},
\end{aligned} \tag{64}$$

$$\begin{aligned}
\bar{T}'_s:\ & t^*=t,\ \ \boldsymbol{x}^*=\boldsymbol{x},\ \ \boldsymbol{r}^*_{(l)}=\boldsymbol{r}_{(l)},\\
& \mathbf{H}^*_{\{n\}}=\mathrm{e}^{k_s}\mathbf{H}_{\{n\}},\ \ \mathbf{I}^*_{\{n\}}=\mathrm{e}^{k_s}\mathbf{I}_{\{n\}},
\end{aligned} \tag{65}$$

all of which are of purely statistical nature. Subsequently, we will call them statistical symmetries. In the translation of the relative coordinates (63) $\boldsymbol{k}_{(l)}$ represents the related set of group parameters. Note that this group is not related to the classical translation group in usual $\boldsymbol{x}$-space (here T_7-T_9 in equation (60) with $\boldsymbol{f}=const.$).

The second set of statistical symmetries (64) was in fact already partially identified in [9], however, mistakenly taken for the Galilean group. In the above general form it was identified in [1] where $\mathbf{C}_{\{n\}}$ and $\mathbf{D}_{\{n\}}$ refer to group parameters and further extended in [2], so that $\mathbf{C}_{\{n\}}$ is a function of time $\mathbf{C}_{\{n\}}(t)$ and then a temporal derivative of $\mathbf{C}_{\{n\}}$ appears also for the transformation of $\mathbf{I}^*_{\{n\}}$.

It is considered that Kraichnan [11] recognised this first. He observed the first element of the infinite set of symmetries in (64), which is in fact valid for the mean velocity, i.e. $\bar{\boldsymbol{U}}^* = \bar{\boldsymbol{U}} + \boldsymbol{C}$ and which he named random Galilean invariance.

It is essentially this latter statistical group that is one of the key ingredients for the logarithmic law of the wall which in fact constitutes a solution of the infinite set of MPC equations to be shown below.

The third statistical group (65) that has been identified denotes simple scaling of all MPC tensors.

Furthermore there exists at least one more symmetry, which consists of a combination of multi-point velocity and of pressure-velocity correlations [see 2]. Its concrete form is omitted at this point because it is not needed for the further considerations.

It should finally be added that due to the linearity of the MPC equation (22) another generic symmetry is admitted. This is in fact featured by all linear differential equations [see 5]. It merely reflects the super-position principle of linear differential equations though usually cannot directly be adopted for the practical derivation of group invariant solutions.

Transforming (63)-(65) into classical notation we have

$$\begin{aligned}
\bar{T}_1' :\ & t^* = t,\ \boldsymbol{x}^* = \boldsymbol{x},\ \boldsymbol{r}_{(l)}^* = \boldsymbol{r}_{(l)} + \boldsymbol{k}_{(l)},\ \bar{\boldsymbol{U}}^* = \bar{\boldsymbol{U}}, \\
& \bar{P}^* = \bar{P},\ \mathbf{R}_{\{n\}}^* = \mathbf{R}_{\{n\}},\ \mathbf{P}_{\{n\}}^* = \mathbf{P}_{\{n\}}, && (66) \\
\bar{T}_{2_{\{1\}}}' :\ & t^* = t,\ \boldsymbol{x}^* = \boldsymbol{x},\ \boldsymbol{r}_{(l)}^* = \boldsymbol{r}_{(l)},\ \bar{U}_{i_{(0)}}^* = \bar{U}_{i_{(0)}} + C_{i_{(0)}}, \\
& R_{i_{(0)}i_{(1)}}^* = R_{i_{(0)}i_{(1)}} + \bar{U}_{i_{(0)}}\bar{U}_{i_{(1)}} - \\
& \left(\bar{U}_{i_{(0)}} + C_{i_{(0)}}\right)\left(\bar{U}_{i_{(1)}} + C_{i_{(1)}}\right),\ \cdots && (67) \\
\bar{T}_{2_{\{2\}}}' :\ & t^* = t,\ \boldsymbol{x}^* = \boldsymbol{x},\ \boldsymbol{r}_{(l)}^* = \boldsymbol{r}_{(l)},\ \bar{U}_{i_{(0)}}^* = \bar{U}_{i_{(0)}}, \\
& R_{i_{(0)}i_{(1)}}^* = R_{i_{(0)}i_{(1)}} + C_{i_{(0)}i_{(1)}},\ \cdots && (68) \\
\bar{T}_s' :\ & t^* = t,\ \boldsymbol{x}^* = \boldsymbol{x},\ \boldsymbol{r}_{(l)}^* = \boldsymbol{r}_{(l)},\ \bar{U}_{i_{(0)}}^* = \mathrm{e}^{k_s}\bar{U}_{i_{(0)}}, \\
& R_{i_{(0)}i_{(1)}}^* = \mathrm{e}^{k_s}\left[R_{i_{(0)}i_{(1)}} + \left(1 - \mathrm{e}^{k_s}\right)\bar{U}_{i_{(0)}}\bar{U}_{i_{(1)}}\right],\ \cdots, && (69)
\end{aligned}$$

where for the translation symmetry (64) only $n = 1$ and $n = 2$ are presented in (67) and (68). Despite of the fact that each of these groups appear to be almost trivial, since they are simple translational groups in the dependent coordinates, they exhibit an increasingly complexity with increasing tensor order if written in the ($\bar{\boldsymbol{U}}$,$\mathbf{R}$) formulation.

4 Turbulent scaling laws

The visionary and rather classical idea of a turbulent scaling law [see 12] usually refers to two distinct facts:

(i) Introducing a certain set of dimensional parameters such as the wall-friction velocity u_τ or boundary layer thickness Θ to non-dimensionless statistical turbulence variables, for instance the mean velocity, and which in turn leads to a collapse of data if one external parameter is varied such as the Reynolds number.

(ii) An explicit mathematical function is given for statistical turbulence variables such as the mean velocity, Reynolds stresses, etc.

Presently we primarily contemplate with the second definition while the normalisation according to (i) will be introduced on dimensional reasons as well as employing classical arguments. In order to rigorously derive such laws directly from the MPC equations we employ the previously defined idea of a group invariant solution.

It appears to be the driving mechanism for quantities of statistical turbulence which have the strong tendency to establish invariant solutions of the MPC equations while at the same time maximising the number of symmetries involved being limited by the boundary condition.

In the remaining two subsections we adopt the latter condition for the derivation of the accordant invariant solution alternatively later also named turbulent scaling laws, which is the usual phrase in the turbulence literature.

4.1 Near-wall turbulent shear flows

Due to its practical importance wall bounded shear flows are by far, and have been for more than a century, the most intensively investigated turbulent flow. This study employs a vast number of numerical, experimental and modelling approaches.

From all the theoretical approaches the universal law of the wall is the most widely cited and also accepted approach with its essential ingredient being the logarithmic law of the wall. Though a variety of different approaches have been put forward for its derivation neither of them have employed the full multi-point equations, which are the basis for statistical turbulence, nor do they solve an equation that is related to the Navier-Stokes equations.

In the following we demonstrate that the log-law is an invariant solution of the infinite set of multi-point equations and further it is shown that it essentially relies on one of the new symmetry groups (64) or more specifically (67).

Already in [13] it was observed that in the limit of high Reynolds numbers and $|\boldsymbol{r}| \gg \eta_K$ the logarithmic wall law allows for a self-similar solution of the two-point correlation equation (44). This is rather remarkable since for inhomogeneous flows equation (44) is not a partial differential equation in the classic sense but a non-local functional differential equation. Non-locality is denoted by the fact that for a given point $\boldsymbol{x}$ and $\boldsymbol{r}$ not only the dependent variables and derivatives are connected but also terms “at the point” $\boldsymbol{x} + \boldsymbol{r}$ contribute to the equation. In equation (44) this is given by the last term in the first row and the first term in the second row.

Indeed, the terms mentioned above were the major cause for the limitation of the two-point correlation equation to be only applicable to homogeneous flows and, even more challenging, if the Fourier transformed version was considered. In particular the above mentioned non-local terms may not be transformed into Fourier space. It is important to note that this limitation is not present for the symmetry approach.

Within this subsection we exclusively examine wall-parallel turbulent flows only depending on the wall-normal coordinate x_2. Further, we only explicitly write the two-point correlation R_{ij} though all results are also valid for all higher order correlations. This finally yields

$$\bar{U}_1 = \bar{U}_1(x_2), \;\; R_{ij} = R_{ij}(x_2, \boldsymbol{r}), \;\; \dots . \tag{70}$$

With these geometrical assumptions we identify a reduced set of groups. Necessary for the calculation of the subsequent scaling laws are the two scaling groups $\bar{T}_2$ and $\bar{T}_3$ and the translation invariance form $\bar{T}_7 - \bar{T}_9$ in x_2-direction in (62). Additionally, it is necessary to use the above-mentioned statistical symmetries, especially the translational group in correlation space (66), the translational group (67) for $\bar{U}_1$, the translational group (68) for R_{ij} and finally the scaling group (69)

With the known symmetries of the MPC equations we may in a final step generate invariants and as a consequence invariant solutions as have been done for the heat equation above in equation (58). As was noted above the actual calculations may be done invoking infinitesimal transformations [see 5] leading to an equivalent form of the invariance condition.

For the reason of briefness we skip the lengthy computations and obtain the invariance condition for the MPC equation

$$\begin{aligned}
&\frac{\mathrm{d}x_2}{k_2 x_2 + k_{x_2}} = \frac{\mathrm{d}r_{[k]}}{k_2 r_{[k]} + k_{r_{[k]}}} = \frac{\mathrm{d}\bar{U}_1}{(k_2 - k_3 + k_s)\bar{U}_1 + k_{\bar{U}_1}} \\
&= \frac{\mathrm{d}R_{[ij]}}{\xi_{R_{[ij]}}} = \cdots \;\; \text{with} \\
&\xi_{R_{ij}} = (2k_2 - 2k_3 + k_s)R_{ij} - (k_s \bar{U}_1(x_2)\bar{U}_1(x_2 + r_2) + \\
&\quad k_{\bar{U}_1}(\bar{U}_1(x_2) + \bar{U}_1(x_2 + r_2)))\,\delta_{i1}\delta_{j1} + k_{R_{ij}}\,,
\end{aligned} \tag{71}$$

where no summation is implied by the indices in square brackets and instead a concatenation is implied where the indices are consecutively assigned its values. For brevity explicit dependencies on the independent variables are only given where there is an unambiguity. Any solution of (71) for an arbitrary set of parameters k_i generates a set of invariants which are in fact invariant solutions and hence if implemented into the MPC equation leads to a symmetry reduction, similar to the heat equation example in (55)-(59).

In fact, with a distinct combinations of parameters k_2, k_3 and k_s a multitude of flows may be described where here we first focus on the log-law. We may keep in mind that $\bar{U}_1$ exclusively depends on x_2 and not on $\boldsymbol{r}$.

Considering the classic case of the logarithmic wall law the reason of the appearing symmetry breaking can be found by revisiting the key idea of von Kármán. He assumed that close to the wall the wall-friction velocity u_τ is the only parameter determining the flow. This condition causes a symmetry breaking of the scaling of the velocity. In order to comprehend this we combine three admitted scaling groups of the MPC equation (32), i.e. $\bar{T}_2$ and $\bar{T}_3$ in (62) and $\bar{T}_s'$ in (69), which leads to

$$\bar{U}_1^* = \mathrm{e}^{k_2 - k_3 + k_s}\bar{U}_1 \;\; , \tag{72}$$

where all other variables have been omitted for clarity. As u_τ is a velocity scale, it acts as some kind of external constraint on the flow and hence, velocities are no longer scalable, which results in

$$k_2 - k_3 + k_s = 0 \tag{73}$$

[see 1].

Under this assumption (71) leads to the extended classical functional form of the mean velocity

$$\bar{U}_1 = \frac{k_{\bar{U}_1}}{k_2} \ln\left(x_2 + \frac{k_{x_2}}{k_2}\right) + C_{\mathrm{log}}, \tag{74}$$

where C_{log} in (74) is a constant of integration.

Obviously equation (74) is a slightly generalised form of the classic logarithmic wall law since the term $\frac{k_{x_2}}{k_2}$ induces a possible displacement of the origin. In its dimensionless form it reads

$$\bar{U}_1^+ = \frac{1}{\kappa}\ln(x_2^+ + A^+) + C \;\; . \tag{75}$$

Moreover, the invariant solutions for the two-point correlations (not shown here) can be reduced to Reynolds stresses by taking the limit $r \rightarrow 0$ so that we gain

$$\begin{aligned}
\overline{u_i u_j}^+ &= D_{ij}(x_2^+ + A^+)^\gamma + A_{ij} + B_{ij}x_2^+\,, \quad ij \neq 11 \\
\overline{u_1 u_1}^+ &= D_{11}(x_2^+ + A^+)^\gamma - \frac{1}{\kappa^2}\ln^2(x_2^+ + A^+) \\
&\quad + \sigma\ln(x_2^+ + A^+) + A_{11} + B_{11}x_2^+
\end{aligned} \tag{76}$$

where the new constants σ, A_{ij}, B_{ij} and D_{ij} are combinations of the k_α in the symmetries (62)-(66). Of course, κ is the same constant in all higher moments, so that the main behavior of these scaling laws only depends on a reduced set of parameters.

Both the mean velocity (75) and the stresses (76) are compared to the DNS data of [14] in the near-wall region of a turbulent Poiseulle flow (see Figure 1) where the mean velocity is in Figure 2 and the stresses are given in Figure 3.

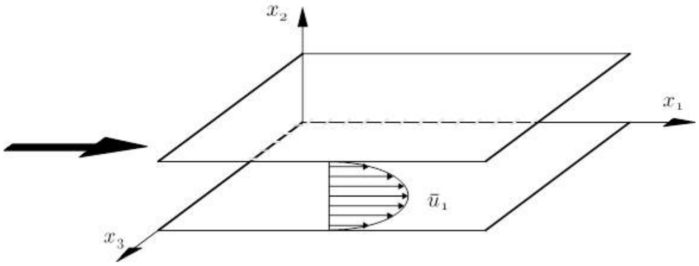

Figure 1. Flow geometry of the pressure driven channel flow.

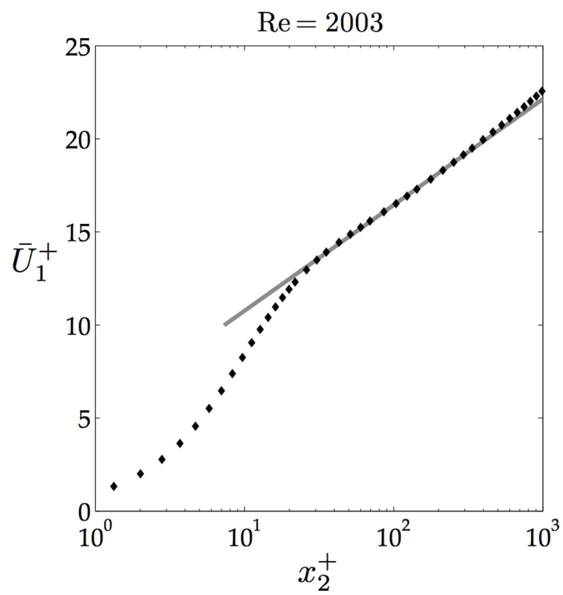

Figure 2. Comparison of DNS data $(\cdots)$ [14] with the log-law (75) with $\kappa = 4.05$, $B = 5.07$ and $A^+ = 0$ $(-)$ for the averaged velocities.

4.2 Non-rotating and rotating channel flow

The second application considered is the rotating channel flow, where, besides the classical non-rotating case, different rotational axes are considered.

Using our symmetry analysis to gain scaling laws, the calculated symmetries have to be transformed into the coordinate system of a rotating frame [see e.g. 3]. Then the invariant system can be developed and for each rotational axis the symmetries must be determined.

This leads to a rather complex and involved form of the operator (71) so details have to be omitted and only results for the mean flow will be given. In the present sub-section we consider two cases of a rotating channel i.e. rotation about the x_2 and about the x_3 axis.

We first assume that the rotational axis lies along the x_3 direction i.e. only Ω_3 is non-zero. Applying Lie symmetry analysis the classical symmetries i.e. scaling in space and the Galilei invariance are used and they are extended by the action of the new scaling symmetry (69) and the translation of the velocities (67).

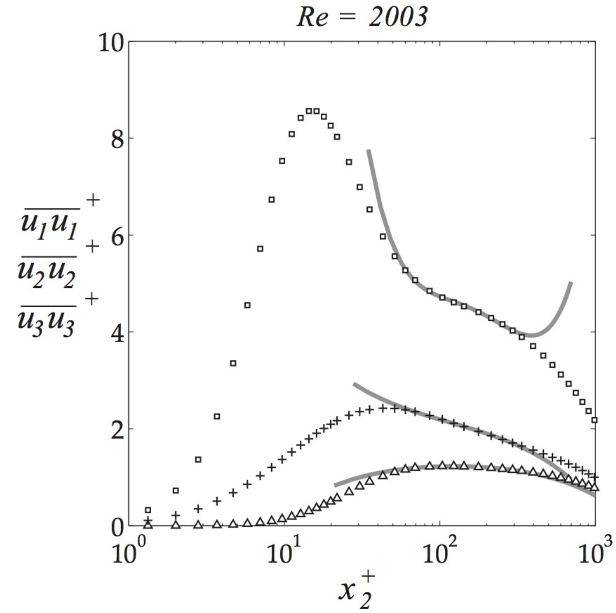

Figure 3. Comparison of DNS data $(\cdots)$ [14] with our analytical results (76) $(-)$ for the Reynolds stress tensor.

Solving the resulting system for the invariant solution, we gain an exponential type of solution which in normalised form reads

$$\frac{\bar{U}_1(x_2) - \bar{U}_{cl}}{\Omega_3 h} = A(Ro_2)\left(\mathrm{e}^{\gamma(Ro_3)x_2/h} - 1\right), \tag{77}$$

where $A(Ro_3)$ and $\gamma(Ro_3)$ are unknown functions of the rotation number $Ro_3 = \frac{2\Omega_3 h}{U_b}$, though its functional form has not been determined from symmetry theory. U_b and $\bar{U}_{cl}$ are respectively bulk and center line velocity. $\gamma(Ro_3)$ converges to zero for increasing Ro_3 while $A(Ro_3)$ tends to a constant in this limit. Carrying out the latter limit $Ro_3 \to \infty$ we obtain the well-known scaling law for a rotating channel about the x_3-axis [see 15]

$$\bar{U}_1(x_2) = A_\infty \Omega_3 x_2 + \bar{U}_{cl}\,. \tag{78}$$

A clear validation of (77) and (78) is given in Figure 4 for various Ω_3 taken from the DNS of [16]. Interesting enough the value for A_∞ appears to be very close to 2.

As the stresses are not available from the literature but the corresponding kinetic energy (formulas may be taken from [3]) are shown in Figure 5.

Next, assuming rotation about x_2, two velocity components $\bar{U}_1$ and $\bar{U}_3$ have to be taken into consideration since the Coriolis force induces a cross flow. Again, both averaged velocities may only depend on x_2. Different to the first case is that one additional symmetry appears, namely translation in time i.e. $\bar{T}_1'$ in

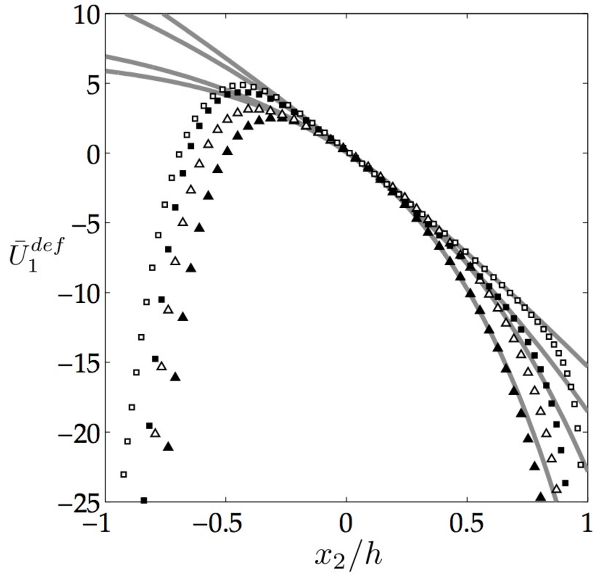

Figure 4. Comparison of the mean velocity scaling law (−) in (77)/(78) with the DNS data ($\cdots$) of [16] at rotation rates $Ro_3 = 0.1,\ 0.15,\ 0.2,\ 0.5$ and $Re_\tau = 194$.

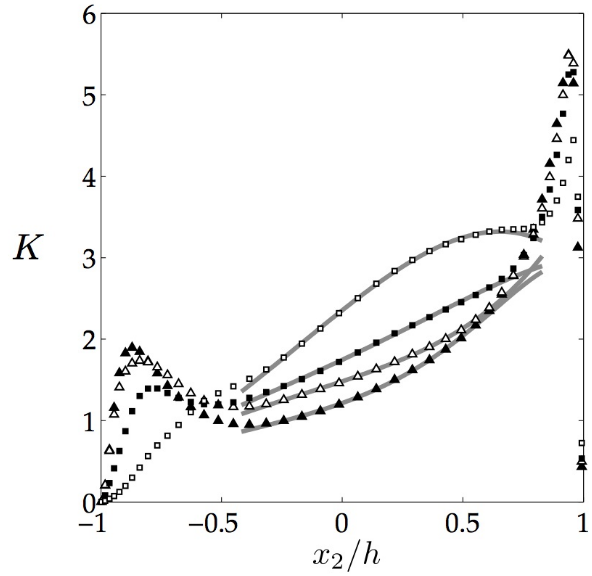

Figure 5. Comparison of the kinetic energy scaling (−) with the DNS data ($\cdots$) of [16] at rotation rates $Ro_3 = 0.1,\ 0.15,\ 0.2,\ 0.5$ and $Re_\tau = 194$.

(63). From this we derive the new Ω_2 depending scaling laws

$$\frac{\bar{U}_1}{u_\tau} = \left(\frac{y}{h}\right)^b \left[a_1 \cos\left(cRo_2 \cdot \ln\frac{y}{h}\right) + a_2 \sin\left(cRo_2 \cdot \ln\frac{y}{h}\right)\right] + d_1(Ro_2)$$
$$\frac{\bar{U}_3}{u_\tau} = \left(\frac{y}{h}\right)^b \left[a_1 \sin\left(cRo_2 \cdot \ln\frac{y}{h}\right) - a_2 \cos\left(cRo_2 \cdot \ln\frac{y}{h}\right)\right] + d_2(Ro_2)\,. \tag{79}$$

with $Ro_2 = \frac{2\Omega_2 h}{u_{\tau 0}}$. A first comparison to DNS data is done for the non-rotating case. Here we employ the DNS data of [14] at $Re_\tau = 2003$ and compare them with the scaling law (79a) at $Ro_2 = 0$, which then maybe rewrittent in defect scaling to obtain

$$\frac{U_{cl} - \bar{U}_1}{u_\tau} = a\left(\frac{y}{h}\right)^b \tag{80}$$

where U_{cl} is the velocity at the center of the channel and u_τ is the friction velocity. Figure 6 shows an almost perfect agreement of the scaling law (80) with the latter DNS where the parameters are fitted to $a = 6.43$ and $b = 1.93$.

For the non-rotating cases the stresses computed from the above symmetries (62)-(66) have a rather compact form and we give them here as an example

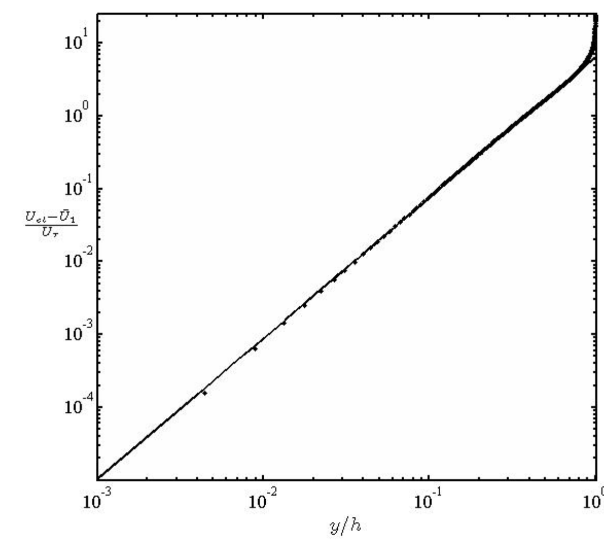

Figure 6. Comparison of the mean velocity scaling law (−) in (80) with the DNS data ($\cdots$) of [14] at $Re_\tau = 2003$.

$$\overline{u_i u_j}^+ = \tilde{D}_{ij}\left(\frac{x_2}{h}\right)^{b-1} + \tilde{A}_{ij} + \tilde{B}_{ij}\frac{x_2}{h}, \quad ij \neq 11$$
$$\overline{u_1 u_1}^+ = \tilde{D}_{11}\left(\frac{x_2}{h}\right)^{b-1} - a^2\left(\frac{x_2}{h}\right)^{2b} + \tilde{\sigma}\frac{U_{cl}}{u_\tau}\left(\frac{x_2}{h}\right)^b + \tilde{A}_{11} + \tilde{B}_{11}\frac{x_2}{h} \tag{81}$$

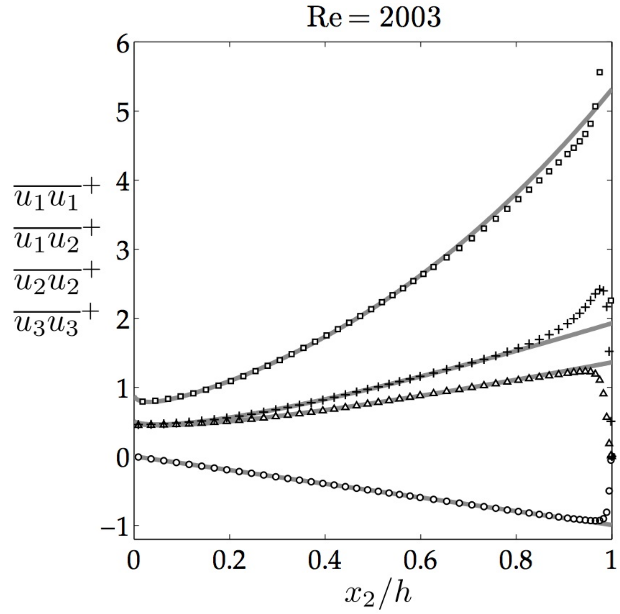

Figure 7. Comparison of the turbulent stress scaling law (−) in (81) with the DNS data $(\cdots)$ of [14] at $Re_\tau = 2003$.

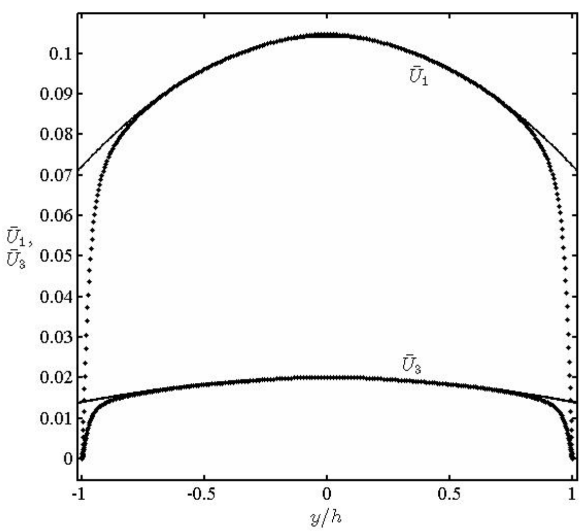

Figure 8. Comparison of the scaling law (−) in (79) with the DNS data $(\cdots)$ of [17] at $Ro_2 = 0.011$.

and compare them to the above given DNS data by [14] in Figure 7.

For the rotating case $Ro_2 \neq 0$ we compare the DNS data of [17] at $Re_\tau = 360$ with the scaling law (79). Results are depicted for two different rotation numbers Ro_2 defined below equation (79) in the Figures 8 and 9 exhibiting an excellent fit in the center of the channel for all cases. $u_{\tau 0}$ refers to the friction velocity of the non-rotating case. It is to note from all the DNS data sets

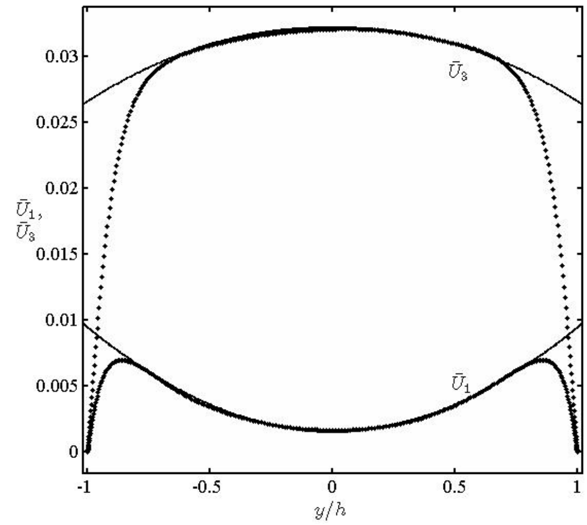

Figure 9. Comparison of the scaling law (−) in (79) with the DNS data $(\cdots)$ of [17] at $Ro_2 = 0.18$.

in [17] we find that with an increasing Ω_2 the magnitude of $\bar{U}_1$ and $\bar{U}_3$ switch position since with increasing rotation rates $\bar{U}_1$ is suppressed while $\bar{U}_3$ increases up to a certain point and decreases again though to a smaller extend compared to $\bar{U}_1$. This behavior is exactly described by the scaling law (79). Because of its complexity the corresponding stresses have been omitted.

4.3 Channel flow with constant wall transpiration

The final setting to be investigated is a turbulent Poiseulle flow with constant wall transpiration, i.e. blowing and suction at the lower and upper wall respectively. Subsequently we show that the transpiration velocity is symmetry breaking, rather similar to the near-wall mechanism at the wall where u_τ breaks the scaling symmetry of velocity pointed out below (72) and which in turn implied the classical near-wall log-law. In the present case the constant transpiration velocity v_0 implies a logarithmic scaling law in the core of the channel and a set of DNS runs validated this result of Lie symmetry analysis and further aided to establish a new logarithmic law of deficit-type of the form

$$\frac{\bar{U}_1 - U_B}{u_\tau} = \frac{1}{\gamma} \ln\left(\frac{x_2}{h}\right). \qquad (82)$$

Further, it is not only the region of validity of the new logarithmic law which is very different from the usual near-wall log-law but also the slope constant in the core region differs from the von Kármán constant κ and is equal to $\gamma = 0.3$.

5 Summary and outlook

Within the present contribution it was shown that the admitted symmetry groups of the infinite set of multi-point correlation

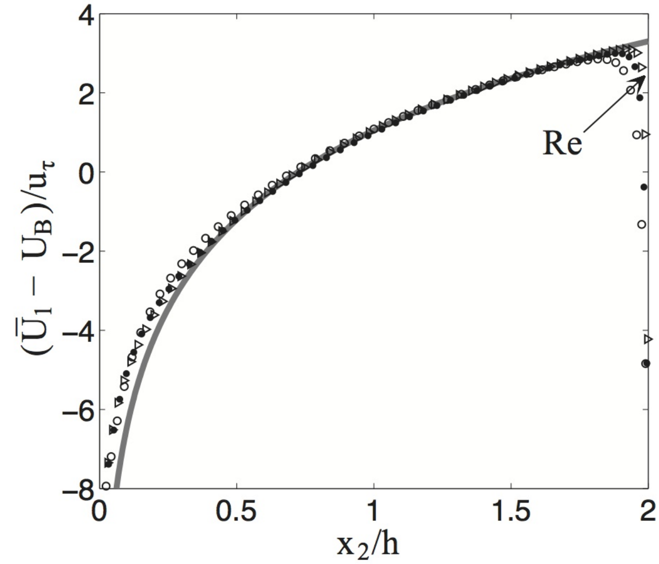

Figure 10. Mean velocity profiles at constant transpiration rate $v_0^+ = 0.16$: ∘, $Re_\tau = 250$; •, $Re_\tau = 480$; ▷, $Re_\tau = 850$ vs. the scaling law (82).

equations are considerable extended by three classes of groups compared to those originally stemming from the Euler and the Navier-Stokes equations. In fact, it was demonstrated that it is exactly these symmetries which are essentially needed to validate certain classical scaling laws such as the log-law from first principles and also to derive a large set of new scaling laws.

Implicitly, symmetries have been used in turbulence modeling for several decades since essentially all symmetries of Euler and the Navier-Stokes equations have been made part of modern turbulence models. Still, this is only partially true for the new statistical symmetries. In fact, some of them have been employed even in very early turbulence models since many of them where calibrated against the log-law. Many other symmetries, however, have never been made use of and in fact, it might be even impossible to make turbulence models consistent with some of the symmetries such as the new scaling symmetry (65).

Still, even with these new symmetry groups at hand which give a much deeper understanding on turbulence statistics there are still some key open questions to be answered. (i) So far completeness of all admitted symmetries of the MPC equation has not been shown. This appears to be necessary not only from a theoretical point of few but rather essential to generate scaling for all higher moments. (ii) From turbulence data it is apparent that the appearing group parameters do have certain decisive values which are to be determined. In some very rare cases such as the classical decaying turbulence case values such as the decay exponent may be determined from integral invariants. Still, a general scheme is unknown. (iii) Finally, we clearly observe that certain scaling laws such as the log law only cover certain regions of a turbulent flow and are usually embedded within other layers of turbulence. Still, the matching of turbulent scaling laws is still an open question.

An apparent extension of the presented machinery to turbulent hear transfer problems is achieved by adding the scalar heat transfer equation to the Navier-Stokes equations (1), (2). This might be either in the most simple case a passive temperature equation or, if buoyancy is considered, the temperature equation again, while the momentum equation (2) is extended by the Boussinesq approximation. In both cases, the multi-point system (22) is extended by an additional tensor composed of the temperature correlated with m velocities, where $m = 1, \dots, \infty$. Note, that because of the linearity of the temperature equation and the linearity of the temperature in the momentum equation due the Boussinesq approximation, it is not necessary to derive correlations and equations which contain the temperature more than once.

Other extension such as to Navier-Stokes equations for compressible fluids, i.e. the gas dynamics equations prolonged by viscous terms, are less forward. The reason is that a correlation tensor of density and velocities may be defined rather straight forward, the corresponding equation may only contain terms, where density and one of the velocities are at the same point. Additionally, the situation is further complicated by the fact, that an energy equation is coupled in which may also gives rise to tensors, that may in principle be defined but the corresponding equation may only contain terms, where energy and one of the velocities are at the same point.

Finally, depending on the Mach number Ma, the gas-dynamics equations may change type and hence, for $Ma > 1$ correlations may only be uniquely defined within the Mach cone. This, apparently, posses an additionally non-trivial constraint on the problem which is unsolved to date.

REFERENCES

[1] M. Oberlack and A. Rosteck, "New statistical symmetries of the multi-point equations and its importance for turbulent scaling laws," *Discrete Contin. Dyn. Sys., Ser. S*, Vol. 3, pp. 451–471, 2010.

[2] A. Rosteck and M. Oberlack, "Lie algebra of the symmetries of the multi-point equations in statistical turbulence theory," *J Nonlinear Math. Phys.*, Vol. 18, pp. 251–264, 2011.

[3] A. M. Rosteck, *Scaling Laws in Turbulence - A Theoretical Approach Using Lie-Point Symmetries*. PhD thesis, TU Darmstadt, 2013.

[4] L. Keller and A. Friedmann, "Differentialgleichungen für die turbulente Bewegung einer kompressiblen Flüssigkeit," *Proc. First. Int. Congr. Appl. Mech.*, pp. 395–405, 1924.

[5] G. Bluman, A. Cheviakov, and S. Anco, *Applications of Symmetry Methods to Partial Differential Equations*. New York: Springer-Verlag, 2010, Vol. 168 Appl. Math. Sci.

[6] V. V. Pukhnachev, "Invariant solutions of Navier-Stokes equations describing motions with free boundary," *Dokl. Akad. Nauk*, Vol. 202, p. 302, 1972.

[7] V. K. Andreev and A. A. Rodionov, “Group analysis of the equations of planar flows of an ideal fluid in Lagrange coordintes,” *Dokl. Akad. Nauk SSSR*, Vol. 298, pp. 1358–1361, 1988.

[8] B. J. Cantwell, “Similarity transformations for the two-dimensional, unsteady, stream-function equation,” *J. Fluid Mech.*, Vol. 85, pp. 257–271, 1978.

[9] M. Oberlack, *Symmetrie, Invarianz und Selbstähnlichkeit in der Turbulenz*. Habilitation thesis, RWTH Aachen, 2000.

[10] J. Khujadze and M. Oberlack, “DNS and scaling laws from new symmetry groups of ZPG turbulent boundary layer flow,” *Theoret. Comput. Fluid Dyn.*, Vol. 18, pp. 391–411, 2004.

[11] R. H. Kraichnan, “Lagrangian history closure approximation for turbulence,” *Phys. Fluids*, Vol. 8, pp. 575–598, 1965.

[12] S. B. Pope, *Turbulent Flows*. Cambridge: Cambridge University Press, 2000.

[13] M. Oberlack, “Analysis of the two-point velocity correlations in turbulent boundary layer flows,” in *Annual Research Briefs*, Center for Turbulence Research, Stanford University/NASA Ames, CA, USA, 1995, pp. 209–220.

[14] S. Hoyas and J. Jimenez, “Scaling of velocity fluctuations in turbulent channels up to $Re_\tau = 2000$,” *Phys. of Fluids*, Vol. 18, p. 011702, 2006.

[15] M. Oberlack, “A unified approach for symmetries in plane parallel turbulent shear flows,” *J. Fluid Mech.*, Vol. 427, pp. 299–328, 2001.

[16] R. Kristoffersen and H. I. Andersson, “Direct simulations of low-Reynolds-number turbulent flow in a rotating channel,” *J. Fluid Mech.*, Vol. 256, pp. 163–197, 1993.

[17] A. Mehdizadeh and M. Oberlack, “Analytical and numerical investigations of laminar and turbulent Poiseuille-Ekman flow at different rotation rates,” *Phys. of Fluids*, Vol. 22, p. 105104, 2010.